Received: 3 July 2022 | Revised: 16 December 2022 | Accepted: 22 December 2022

DOI: 10.1002/rra.4101

RESEARCH ARTICLE

WILEY

Ship waves in rivers: Environmental criteria and analysis methods for measurements

John D. Fenton[1] | Boris Huber[1] | Gerhard Klasz[2] | Norbert Krouzecky[1]

[1]Institute of Hydraulic Engineering and Water Resources Management, TU Wien, Vienna, Austria

[2]Hydraulic Engineering and Water Management, Vienna, Austria

Correspondence
John D. Fenton, Institute of Hydraulic Engineering and Water Resources Management, TU Wien, Karlsplatz 13/222, Vienna, 1040, Austria.
Email: johndfenton@gmail.com

Abstract

A literature review shows that the most important physical quantities determining environmental impact of ship waves in a waterway are the fluid velocities, maximum and minimum water levels, and size of drawdown events. Fluid velocity can vary strongly in the vertical so that the usual measurements at a single point are not enough unless made near where the effects are most important, often the bed. Customary use of wave height as a measure of impact has been misleading, because the all-important fluid velocity is of a scale given by wave height divided by wave period. A good and simple estimate of the surface velocity as a disturbance scale is shown to be given by the time derivative of the free surface height. The most important role of linear wave theory is to explain and understand the physics and measurement procedures, such as done here in several places. Its use for obtaining numerical results is criticised. Instead, three integral measures of impact are proposed, all of which use surface elevation measurements and which require no essential mathematical approximations or wave-by-wave analysis. The methods are applied to a study of ship waves on the Danube River. A number of results are presented, including examination of the effects of measurement frequency. After a ship passage, due to repeated shoreline reflections of the wake waves, the river is brought into a long-lasting state of short-crested disturbances, with finite fluid velocities. The environmental consequences of this might be important. After the primary and secondary ship waves it could be called the tertiary wave system.

KEYWORDS

anthropogenic disturbances, Danube, environmental criteria, field measurements, inland navigation

1 | INTRODUCTION

In a seminal study of ship-induced waves, Bhowmik, Demissie, and Osakada (1981) listed their physical effects, but not biological ones. In the intervening 40 years, the natural environment has come to be considered more important. Gabel, Lorenz, and Stoll (2017) presented an encyclopaedic review of the effects of ship-induced waves on aquatic ecosystems, based on more than 200 publications. Reading that review it is possible to identify that almost every biological impact was a consequence of at least one or more of three physical quantities:

- The fluid velocity due to the waves, where a critical instantaneous value might be important in uprooting or damaging plants; causing sediment re-suspension, shoreline erosion and turbidity; and dislodging animals, their eggs, or their nests from the bed and its vegetation. Sustained higher and variable velocities can cause difficulties for swimming animals.
- Sudden inundation and draining of the banks and nearshore zone, leading to stranding of animals and washing away of eggs and nests.
- Magnitude and duration of the exposure of the river banks due to drawdown, leading to longer-term stranding and erosion.

With those quantities in mind, here the previous literature on ship waves in rivers and lakes is examined, to consider the quantities measured, relationships obtained, and conclusions drawn. It is found that there have been few general scientific results obtained. Some wave theory will be used to help determine what the important quantities are, and what could be measured better, or in one important case, the pressure, best not used at all. However, it is recommended strongly that, while simple approximate theory can be used for understanding and insight, it is not adequate for the accurate calculation of numerical results.

As velocity varies strongly with vertical position, single-point measurements often do not have much relevance. It is shown that measurements of the free surface elevation can be implemented, used, and analysed relatively simply to give information about the physical effects of ship waves, including the magnitude of fluid velocity. Several numerical techniques are proposed, which are then tested by application to a number of measurements of waves from vessels on the Danube River east of Vienna.

2 | LITERATURE REVIEW

Considering experimental techniques, surface elevation is the easiest quantity to measure. Some investigators have used a vertical staff gauge or even a board inclined parallel to the bank, in association with a video camera. However most found more direct electronic methods better, such as capacitance wave gauges or acoustic wave sensors, where higher frequency readings can be taken. Several investigators obtained it from underwater pressure measurements. Some did not describe how these were converted to surface height. Others clearly used the transfer function from linear wave theory. However, there are severe problems associated with such measurements of short high ship waves, which will be described in Section 2.1.2. For fluid velocity measurements, conventional slow-response current meters are not adequate. Acoustic Doppler velocimeters or electromagnetic flow meters for point measurements have been used successfully; acoustic Doppler current profilers give more information, although where velocity is most important and varies rapidly, near the bed, they have limited application. Considering turbidity and suspended solids, surface scatter turbidimeters and acoustic velocity and backscatter intensity measurements have been implemented.

The approaches that have been taken to the processing of the experimental results will now be described and analysed. In most cases, wave-by-wave analyses have been carried out and crest and troughs identified to give, for each wave, a height H and often a corresponding period T. Considering all the waves of an event separately, the notations $H_{\max}$, and $T_{\max}$ are obvious. Then, when all waves in a record are considered, the mean wave height $\overline{H}$ can be calculated, as can the significant wave height H_s, the average wave height of the highest one-third of the waves. In the survey, if the total energy or mean power transmission rate of all the waves has been calculated, that is noted. Finally, it is shown where any overall numerical conclusions and correlations have been made. No mention is made here where numerical results are given without such deductions. A critique of the quantities that have been used to parameterise the problem is presented in Section 2.1.

Occasional use will be made of the terms *primary* wave to describe the long-period drawdown wave typically surrounding a displacement craft and *secondary* waves for the commonly observed system of diverging and transverse oscillatory waves, also called the *ship wave pattern*.

Bhowmik et al. (1981) analysed waves generated mostly by push-tow-barge assemblies in two large rivers. Values of $H_{\max}$ were calculated. They observed that with such vessels, the maximum change in water surface elevation during a drawdown $D_{\max}$ was the most important quantity. Values were presented, but it is not clear how they were calculated, in the presence of many shorter waves. Poor agreement of both $H_{\max}$ and $D_{\max}$ with empirical formulae was noted. It was suggested that the total drawdown period and the extent of shoreline exposure and its duration might be more important in bank erosion and biological studies.

Bhowmik, Soong, Reichelt, and Seddik (1991) studied waves due mostly to small recreational boats on a large river. They obtained the height H, period T, and what they called the “steepness” H/T of each individual wave, but that was not subsequently used. Then they calculated maximum and average wave heights, $H_{\max}$ and $\overline{H}$, total event duration, number of waves, the significant wave height H_s, as well as the wave energy. They developed empirical relationships for $H_{\max}$ and H_s for use on that river.

Nanson, von Krusenstierna, Bryant, and Renilson (1994) also used wave-by-wave analysis to give $H_{\max}$, plus statistics from the whole record to give H_s and $\overline{T}$, from which mean wavelength $\overline{L}$ was calculated using a deep-water formula. Mean power parameters were calculated from linear deep-water formulae for $H_{\max}$ and H_s. An innovation was the calculation of wave steepness $H_{\max}/\overline{L}$. Three erosion indices were measured, which showed a strong correlation with all the wave characteristics except, surprisingly, for wave steepness. It is possible that that is because they calculated the length from a deep-water formula. They gave an interesting physical discussion of quantities that take into account the whole wave train ($\overline{T}$, $\overline{L}$, H_s, and significant wave power) and those that describe only part of the wave train ($H_{\max}$, peak wave power, and $H_{\max}/\overline{L}$). In the end, simply $H_{\max}$ was found to be the most convenient variable to predict erosion because “it had a well-defined threshold and was easy to measure”.

The quantities characteristic of the wave train as a whole did not give a significantly better level of explanation.

Sorensen (1997) gave a critical analysis of all the factors governing ship waves, especially the maximum wave height, noting all the difficulties mentioned elsewhere here and the difficulties of defining energy, especially considering length of wave record. He considered nine wave height models for calculating $H_{\max}$, but noted that only three satisfied the applicability criteria that he set out. They were applied to data mainly from recreational vessels on the Upper Mississippi River System. It was concluded that "most of the models have limited application. The limited data available to evaluate these models show significant scatter and are deficient in the available supporting information on vessel hull characteristics."

McConchie and Toleman (2003) used Fourier analysis of pressure signals to separate motorboat waves from wind waves, and they measured suspended sediment concentrations as indicative of the erosion potential of the waves. Then they used a combination of information from the Fourier analysis and wave-by-wave analysis to produce results in terms of wave amplitude rather than wave height (one is half the other for a pure sine wave, but not for a finite-amplitude water wave). They also gave an interesting discussion of the relevance of local peak and general quantities. They too, in principle inclined towards quantities characteristic of the whole wave train. They calculated them, including number of waves, duration, and total energy, but found difficulty in determining the exact length of the wake train. Hence they also just used maximum amplitude and calculated the period of that wave and its energy, again using linear wave theory. They measured at several places, finding the results to be highly site specific, with little meaningful correlation of results with variables presented.

Maynord (2005) studied wave heights generated by planning and semi-planning small boats on a lake. The data for $H_{\max}$ obtained seem to come from a wave-by-wave analysis. Two conditions were studied, one was the wave generated when the boat was at maximum power, and the other was the maximum wave height over all boat speeds. Several of the later references below cite Maynord's use of $H_{\max}$ as innovative and definitive. It was not, as the above earlier citations show—it was the only quantity for which he provided results. A wave height equation was developed for the type of boats studied, based on boat speed, volume displaced by the boat, and distance from the shore.

Gabel et al. (2008) conducted experiments in a small wave tank with a single-throw flap wavemaker that generated a solitary wave. Trays of five different habitats (coarse woody debris, reeds, sand, stones, and tree roots) were arranged behind a near-bed velocimeter, and for each run, 20 individuals were introduced and habituated, each of five different benthic organisms "selected because they differ considerably in body shape, locomotion behaviour and attachment strategies, all of which should influence their sensitivity to wave impact". The number of individuals subsequently detached from each habitat was measured from the analysis of video records. The measure of the disturbance to the creatures was the shear stress τ on the bottom, calculated from the formula $\tau = \frac{1}{2}\rho f_w U_b^2$, where ρ is fluid density, U_b is the maximum fluid velocity measured, and f_w is the wave resistance coefficient, for which the authors used a formula valid for laminar flow, obtained from linear periodic wave theory. For the different habitats and boundary textures in the experiments, there would have been a quite different friction factor. It would have been more fundamental to have used the measured velocity tending to detach the organisms rather than a stress calculated in this approximate manner. Among the conclusions was "results showed that detachment of invertebrates was significantly related to shear stress in all habitats except tree roots".

Hofmann, Lorke, and Peeters (2008) considered waves due to wind and passenger vessels in a large lake. They measured pressure at about half the depth and used Fourier analysis to obtain surface height from pressures using the transfer function from linear wave theory. The procedure is fraught with problems as will be described below. All measurements were analysed in bursts. They also measured the "near-bottom" velocity and turbidity just above the bottom. Values of $H_{\max}$, H_s, and T_s were calculated by wave-by-wave analysis. The wave heights were calculated using twice the amplitude of the wave, determined to be the difference between the maximum elevation of one wave and the mean of the elevation in the burst period. That is not quite correct for finite-amplitude waves. The maximum current velocity on the bed was calculated from the maximum wave height using linear wave theory and similarly so were wave energy and its flux. They observed that "distinct peaks in $H_{\max}$ generated by ship waves are correlated with peaks in turbidity, which makes it evident that the occurrence of ship waves causes resuspension".

Kucera-Hirzinger et al. (2008) conducted measurements in the Danube River east of Vienna, considering three different shoreline types. Records were obtained of surface height every 15 s, water velocity every 2 s, and turbidity. Few details of the analysis were given. Hydrofoils and excursion ships had significantly higher waves, while cargo vessels and large sports boats had the smallest impact. Vessels navigating downstream showed significantly higher waves and water velocities. Several times a critical water velocity was exceeded, defined as such that fish cannot maintain their position for at least 2 min. There were significant increases in suspended solids during ship events, but no significant difference was found between five ship categories. In general, suspended solids concentrations peaked immediately after ship passage and levelled off after 7 min. Besides the concentration of suspended solids, the duration of exposure was stated to be an important factor for the severity of ill effects on fish. It was stated that, although the effects of ships are relatively short, the high frequency of the disturbances on the Danube may cause adverse long-term consequences for fish survival.

Houser (2011) performed a field study to measure sediment re-suspension and transport in response to wakes generated by super-critical pilot boats and sub-critical container ships at the mouth of a large river. A cross-shore transect of five instrument stations was deployed, three with pressure transducers, two with acoustic Doppler velocimeters, pressure transducers, and optical backscatter sensors to measure the amount of re-suspended sediment. Because of the time-varying nature of vessel-generated waves, wavelet analysis, rather than global spectral analysis, was used to describe the results. It was found that the drawdown of the container ships could force a seiche lasting up to an hour, close to the natural resonance period of the river. The identification of wave groups showed that net transport was due to a low-frequency oscillation similar to a second-order group-forced current. Increases in suspended sediment concentration were well described by a function balancing the excess shear stress above the entrainment threshold with the rate of sediment deposition/decay. A lag between the concentration and turbulent kinetic energy level reflected sediment being pumped up through the water column through a wave group.

Gabel, Garcia, Schnauder, and Pusch (2012) explored whether the laboratory results of Gabel et al. (2008) could be observed under field conditions along a natural lake shore affected by waves produced by boats. Again, individuals from five invertebrate species were exposed to waves in five habitats differing in structural complexity. Wave heights were calculated from pressure measurements by a sensor partly buried in the sand, but it was not stated how this was done. As with Gabel et al. (2008), the measure of disturbance was taken to be the shear stress, calculated from velocity measurements. Detachment of benthic invertebrates increased with it. Results showed the effects of boat velocity and distance from the shore, as well as those of habitat complexity.

Liedermann et al. (2014) measured ship waves in the Danube River east of Vienna. Measurements of surface elevations were made in bursts by pressure gauges. Events were classified according to three ship types, large passenger ships, high speed passenger ships, and bulk carriers. The different types showed very different wave characteristics. An analysis comparing wave heights to vessel velocities was performed only for large passenger ships travelling downstream. The much longer transit times for upstream navigating vessels might have caused problems for the data measurement system. It was deduced that "at all bank types, wave heights were found to be rising with absolute ship velocity". The dependence of wave height on the ship distance from the shore was examined for high speed vessels navigating downstream. Wide scatter was found. The conclusion "independent of the shore type, a decreasing wave height with rising distance to the bank was found" was based on a line of best fit, but with a low coefficient of determination. Also for such vessels navigating downstream, the varying bank types and river discharges had a large effect on wave characteristics, with wide scatter of results and conflicting variation with discharge, when results from two different bank types were compared. Some results were presented for drawdown and it was noted that the highest values were observed for slower vessels.

Schludermann et al. (2014) wrote a companion paper to Liedermann et al. (2014). Wave measurements were taken in the same area, using the same pressure gauges. The paper concentrated on the effects of the waves on young fish, notably their drift. More attention was paid to the effects of wetting and drying by measurement of the lateral extent of inundation and exposure by video records coupled with a detailed topographic survey. For selected wave events, the area loss was calculated by subtracting height layers from a detailed digital terrain model. Ship-induced changes in flow velocity were measured. There was no mention of the vertical position of the velocimeter. For the disturbance input to the system, the range (minimum to maximum) of the lateral velocity component was taken; the output was the drift density of young fish, collected in nets. Results were highly dependent on shoreline morphology and slope.

Göransson, Larson, and Althage (2014) studied ships in a river, measuring the water level by means of a video camera directed towards a graduated staff, and turbidity by a surface scatter turbidimeter. Demands of digitisation meant that the focus was on drawdown and maximum secondary wave height. Comparisons were made with common formulae for predicting ship waves. Results for drawdown were evaluated as poor. It was stated that there were no simple relationships available in the literature for the turbidity generated by ship waves. The results showed that it was mainly a function of the observed drawdown, whereas the secondary waves had less impact. The time scale of the turbidity response was much larger than the wave event; thus, typically 30–60 min were needed for the sediment mobilised by the ships to settle. It was observed that accurately predicting ship-generated waves in a restricted waterway is difficult with simplistic formulas, although on average, reasonable accuracy can be obtained if the ship and river properties are known. A more physically based description of the processes governing sediment mobilisation of sediment yielded better predictions of the turbidity, but empirical site-specific coefficients were necessary.

Fleit, Baranya, Krámer, Bihs, and Józsa (2019) gave a comprehensive literature survey. Results were presented from a one-day field measurement campaign on a free-flowing reach of the Danube River upstream of Budapest. They used pressure measurements furthest from the bank to give water levels plus an acoustic Doppler current profiler for the variation of velocity with depth there. Also, three-component single-point velocities were obtained from two acoustic Doppler velocimeters at different distances from the bank. Sophisticated methods were adopted for the processing of experimental data, including de-spiking of acoustic velocity signals and the use of transient spectra based on moving short-run data. The passages of four ships were studied, three passenger vessels and a cargo vessel with a longer event length and larger waves. It was noted that "due to the strong spatial variability, it is clear that single-point velocimetry alone is not sufficient to analyse wave kinematics and its ecological effects in the littoral zone of rivers". A computational fluid dynamics package was described, which solved in two dimensions the Reynolds-averaged Navier–Stokes equations on the irregular domain with surface waves. Velocity spectra from the computational results agreed satisfactorily with those from measurements. Also noted was the need for field and numerical investigation of bank erosion and sediment re-suspension processes. In the conclusions, it was noted that the effects of the different hydrodynamic phenomena on the aquatic fauna are understood, but the quantitative assessment has been barely investigated. Finally, it was suggested that computational methodology might be used to give insights unattainable from field measurements.

Fleit, Hauer, and Baranya (2021) then used the methods and measurements of the previous paper applied to the prediction of habitat use and drift risk of juvenile fish during wave events of different intensities. Results of the hydrodynamic model were combined with data from the literature to explore a case study of a juvenile fish species. Results highlighted the significant horizontal extent (10–15 m) of the region of decreased habitat suitability and increased drift risk.

Fleit and Baranya (2021) also used the experiments described in the previous two papers, here to show that acoustic velocity and backscatter intensity measurements can provide information on ship-wave-induced sediment transport processes. A calibration equation was determined to give suspended sediment concentrations, from which time series were reconstructed. Reasonable overall agreement was observed. Rapid concentration increases as well as gradual settling were observed, showing the sediment re-suspending effect of ship-induced waves. It was noted that the calibration is site specific, and that low-frequency primary waves were more responsible for the lateral sediment transport than the dynamic secondary waves. This will be discussed in the present work. It was noted that the general inhomogeneity of the fluvial environment leads to uncertainties.

Almström, Roelvink, and Larson (2021) conducted a study to test a computer program for predicting waves from conventional maritime vessels. Water level results from two sites in a nearly linear passage through the Stockholm archipelago to the Baltic Sea were obtained from a capacitance probe mounted on existing piers and continuous sampling at 4 Hz. Some of the 42 passages of a conventional vehicular ferry were monitored. In the computer program, the non-linear shallow water equations were combined with a two-layer non-hydrostatic model. The ship was represented by a moving pressure field. Results for drawdown were quite good but not so for the oscillatory secondary system. The necessary hull geometry was noted to be often difficult to obtain, and representing it as a simple pressure field might cause errors. The conclusions stated that the focus was on the primary drawdown wave, the main concern regarding shoreline erosion; however, the results showed that shorter waves induce large velocities, which will be discussed below.

2.1 | Critique

There are relatively few general deductions that can be made from the above survey because conditions (types, speeds, and distances of boats; underwater topography; bank conditions) are so specific to each study that the results obtained are of an inductive nature. While each study successfully fulfilled its own aims, collectively there have been few surprises. Some specific criticisms can be made, as follows.

2.1.1 | Vertical variation of velocity, point measurements, and long wave sediment transport and generation of turbidity

Studies of ship waves have usually measured fluid velocity at one point only, and that point is often at an intermediate vertical position in the water column, rather than near the bed where environmental effects are most important. That is not enough, as will now be shown.

The full three-dimensional velocity field is complicated, although there should be relatively little local change in a streamwise direction. There will be some variation in the transverse onshore direction as the waves feel the bed shoaling, however below in Section 3.5 it will be seen that this is surprisingly small until close to the shore. Considering variation in the vertical, however, the velocity distribution is a function of position, depending strongly on the local wavelengths present. To show this, linear wave theory for two-dimensional steadily progressing waves on a horizontal bed is now used as a model.

Consider a local coordinate system x in the direction of propagation of the waves and z vertically with origin at the mean water level. Expressions for the corresponding fluid velocity components u and w are given by, for example, Dean and Dalrymple (1991, equations 4.3 and 4.5) and Fenton (2015, Section 4.4.2). Surprisingly, neither of those presentations makes clear what the velocity scale is. To do that one can use the dispersion relation (Dean & Dalrymple, 1991, equation 3.52; Fenton, 2015, equation 4.18):

$$\frac{2\pi}{T} = \sigma = \sqrt{gk\tanh kh}\,, \tag{1}$$

where T is period; σ is the angular frequency; g is gravitational acceleration; wavenumber $k = 2\pi/\lambda$, where $\lambda = cT$ is the wave length; and c the wave speed, here ignoring current that would cause some Doppler shifting. Substituting the above variables into the velocity expressions mentioned gives

$$u = \pi\frac{H}{T}\frac{\cosh(k(h+z))}{\sinh kh}\cos(kx-\sigma t), \tag{2a}$$

$$w = \pi\frac{H}{T}\frac{\sinh(k(h+z))}{\sinh kh}\sin(kx-\sigma t), \tag{2b}$$

where H is the crest-to-trough wave height; h is the mean depth; and t is time. This shows that the velocity scale, an important quantity determining environmental impact, is given by H/T, and it is not just the wave height H that is important. Moreover, variation in the vertical is determined for both u and w by ratios of hyperbolic functions, which are functions of k and which take on very different values according to the period of the waves, given by Equation (1). For waves that are long relative to the depth, σ and k are small and there is little variation of horizontal velocity u in the vertical. In the short-wave limit, when the wavelength is less than twice the depth (which would apply up until the last stages of breaking on the banks—see Section 3.5) both hyperbolic function ratios behave like $\exp kz$, which decays very strongly with z negative, down into the water.

The pressure p also shows that strong variation in the vertical. Again using linear wave theory, for example, Dean and Dalrymple (1991, equation 4.22) and Fenton (2015, after equation 4.17):

$$\frac{p}{\rho g} = -z + \frac{H}{2}\frac{\cosh(k(h+z))}{\cosh kh}\cos(kx-\sigma t), \tag{3}$$

where ρ is fluid density. The term with hyperbolic functions shows that the wave-induced pressure, like velocity as seen above, decays down into the fluid, and in the limit of short waves, tends to exponential decay.

The linear solution for free surface elevation is

$$\eta = \frac{H}{2}\cos(kx - \sigma t). \tag{4}$$

If one substitutes $z = \eta$ with that into the expression for pressure, Equation (3), and expands using series operations, one finds that terms cancel and the pressure on the free surface is indeed proportional to H^2, second order, so that at first order the pressure is zero as required. To illustrate the behaviour of the formulae for velocity and pressure, a typical situation is shown in Figure 1, which has been calculated and drawn using the linear wave theory here. As a typical nearshore problem, the physical quantities are a wave of height 15 cm and period 1 s in water of depth 1 m. The wavelength λ, calculated by solving Equation (1) for $k = 2\pi/\lambda$, is about 1.5 m. Shown are the horizontal velocity u profiles under the crest and trough and the pressure head $p/\rho g$ under the crest plotted horizontally; u is plotted to an arbitrary horizontal scale for graphical purposes. The hydrostatic pressure is shown dotted; the total pressure is shown by a solid line. For this wave, corresponding to a quite possible physical situation, the wave is so short relative to depth that variation of velocity and pressure in the vertical is marked. A velocity measurement at any one level is not going to be representative enough, and any measurement of pressure down in the water has to contend with the dominant hydrostatic contribution as well as the marked vertical decay, meaning that inference of surface height from that is difficult, as will be explained below. There can be, in addition, problems of real fluid effects near the bed, where boundary layers modify the local flow, complicated by different types of boundary, whether soil and/or vegetation. The figure incorrectly shows a finite pressure at the crest, which is because the linear wave theory used is not exact (above it was stated how it could be shown to be proportional to H^2), for demonstrative purposes it is satisfactory.

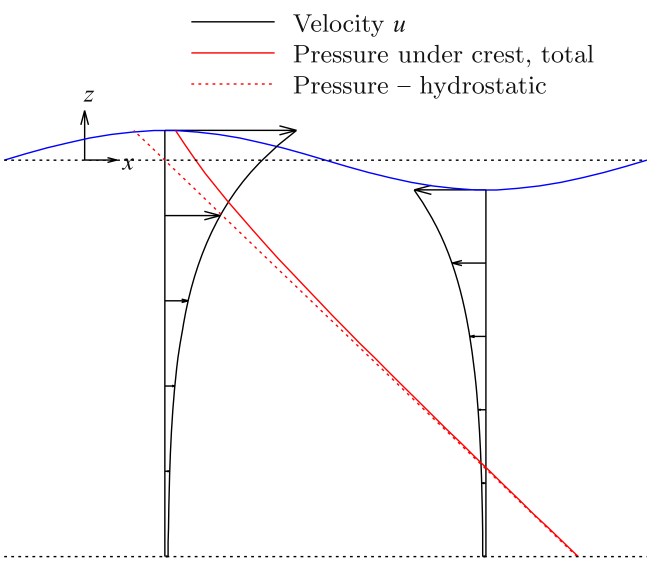

FIGURE 1 A typical nearshore situation—a wave of height 15 cm and period 1 s in water of depth 1 m, modelled by linear theory, showing marked variation of velocity and pressure in the vertical [Color figure can be viewed at wileyonlinelibrary.com]

Not as part of a critique, this is an appropriate place to mention the findings of Houser (2011), Göransson et al. (2014), and Fleit and Baranya (2021), that sediment transport and the generation of turbidity was due to long-period waves, whether due to primary waves (rather than secondary waves), wave groups, and/or seiching. This is explained by the fact that for such long waves, k small, in the formula for horizontal velocity u, Equation (2a), the ratio of hyperbolic functions is 1, showing no decay with depth, and the bed is subject to the same velocity as fluid at the surface, causing initiation of grain movement, transport, and injection into the fluid column. This might be the reason that other researchers, attempting to connect erosion and turbidity with wave period, might have concentrated too much on shorter waves.

2.1.2 | Using pressure measurements to calculate surface elevation

The practice of inferring the water surface level from sub-surface pressure measurements is even more fraught with difficulty. If one had measured a record of pressure and wanted to estimate the corresponding surface heights, the procedure is to calculate the Fourier components P_j of the measured pressure heads corresponding to harmonic frequencies $\sigma_j = j \times 2\pi/T$, where T is the total length of record. Considering Equation (3) to be the jth term of the Fourier series, the surface amplitude coefficient Z_j (corresponding to $H/2$) is given by

$$Z_j = P_j \frac{\cosh k_j h}{\cosh(k_j(h + z_p))}, \tag{5}$$

where z_p is the elevation of the pressure probe and k_j is the wavenumber obtained from the linear dispersion relation, Equation (1), for the harmonic component σ_j. In the limit of short waves, k_j large, the transfer function, the ratio of the hyperbolic functions in Equation (5), varies like $\exp(-k_j z_p)$ which, as z_p is negative down in the water, can be a very large quantity. The results are potentially catastrophic, as the shorter the wave measured is, the much larger is the calculated result. In fact, the problem is even more severe than this suggests, for as k_j becomes large for shorter period components, $\tanh k_j h \to 1$, and Equation (1) shows that the k_j vary like σ_j^2/g, the *square* of the frequency, becoming very large and the hyperbolic functions enormous.

The manufacturer of the gauges used by Liedermann et al. (2014) and Schludermann et al. (2014) was aware of those problems (NIWA, 1998, 2001) and purported to be able to correct for them, although problems were understated ("… the fluctuating pressure is not exactly hydrostatic") and the method of correction was vaguely described. One might be sceptical, as it has not been published and no one else has solved the problem. In any case, a warning is made that "… if you are interested in wave height and period at the surface … you need to deploy … as near to the surface as possible". For short waves such as ship waves the bulk of such a gauge would cause problems near a wave crest. Even if it were submerged just below the wave troughs, the steepness and rapidity of variation in the vicinity of the crests mean that the procedures described above, based on linear theory, would not be accurate.

In addition, there is another important problem with the method of inferring surface height from pressure measurements, which seems never to be addressed. It is that every wave component is assumed to propagate independently at a speed, corresponding to its wavelength, given by the linear dispersion relation, Equation (1). In large waves, strongly non-linear, the main wave component has a number of harmonic waves of shorter wavelength that are bound to it, and travel with the speed of that main wave, faster than if they had been propagating freely. This Doppler shifting will appear in the measured spectrum as an apparent enhanced higher frequency component, where, to obtain the free surface a larger value of frequency corresponding to that would be used, giving a larger contribution to surface elevation than should be the case.

It can be concluded that calculating the free surface elevation reliably and accurately from pressure measurements has marked difficulties.

2.1.3 | Using linear wave theory to calculate results

Linear wave theory is valid for a small not-so-long wave progressing steadily over a flat bed and is a good approximate model to give explanations, in the absence of other information, as has been used above. In many works described in the literature review, however, linear water wave theory was used to obtain numerical results. The accuracy of such calculations is dubious, as in general the waves may not be small, may not be short, and where studied, may not be travelling as two-dimensional waves over a flat bottom. Our opinion is that in the analysis of ship wave measurements, linear wave theory should not be used to obtain numerical results. Below, in Section 3, alternative methods of analysis will be proposed.

2.1.4 | Using wave-by-wave analysis methods

Most of the studies have used a procedure of identifying zero-crossing points of the surface elevation signal and measuring maxima and minima, then considering all of the waves in the signal thus identified. In this way quantities such as $H_{\max}$, $\overline{H}$, $\overline{T}$, H_s, total wave energy, and/or power can be obtained. There is nothing wrong with that, but it is a laborious process and calculations are made difficult by the presence of smaller irregular waves. Different authors noted that it was difficult to identify the length of the wave train caused by a particular vessel.

In any case, as far as environmental quantities are concerned, it is not clear which wave properties are the most important. There are some mechanistic models concerning turbidity. None of the wave measures obtained feature in a mechanistic model of effect on organisms, whether those of an individual wave such as $H_{\max}$, or those of the entire signal, $\overline{H}$, $\overline{T}$, and H_s, energy and power. Some of the references cited discussed this question and emerged with the conclusion that $H_{\max}$ was the simplest quantity and that it was reasonable to use that. The situation is vague.

3 | THE MEASUREMENT OF SHIP WAVES AND PROCESSING OF RESULTS

Here several suggestions are made concerning the importance of different physical quantities and how their magnitude can be estimated by the use of simple methods analysing a single-point gauge measurement of surface elevation. In places linear wave theory will again be used to give explanations of the various problems and their proposed solution; however, following the criticisms of Section 2.1.3, it will not be used to produce numerical results. Instead, simpler methods and formulae are suggested that require no essential approximation.

3.1 | Fluid velocity

In the introduction section, it was observed that the dominant physical quantity in determining effects on the aquatic ecosystem is the fluid velocity. In fact, the various effects mentioned, including the uprooting of plants, dislodging of animals, and re-suspension of sediment could all be modelled by mechanical formulae using a function of the velocity, whether in typical formulae for the drag force on a clinging or swimming animal or the erodibility of bed grains.

It would be best to measure the velocity directly, and near where its physical effects are important for the study, such as among reeds with organisms or close to an erodible bed. However it varies in the vertical in a complicated and possibly strong manner, as was seen in Section 2.1.1, so the measured velocity may not be that causing the effects studied. If the actual velocity is not crucially important to a study and is not measured, two alternatives here give a measure of sub-surface fluid velocities.

3.1.1 | Velocity scale H/T

Throughout the works described in the literature review, the wave heights H obtained from wave-by-wave analyses were considered the main measures of environmental impact, from which other derived quantities such as $H_{\max}$, $\overline{H}$, and H_s were obtained. In view of the deduction here that the dominant physical quantity is actually the fluid velocity, the relevance of H and those derived quantities has to be reconsidered.

Equation (2) for the fluid velocity components show that they are of a scale given by the ratio H/T. It is not suggested to use those equations to calculate them, but they have shown that the wave height H is not necessarily the important quantity in measuring the effect of a single wave on the environment. Rather, as the fluid velocity is important, a better scale to consider is H/T, as environmental effects are largely proportional to a function of velocity.

In a compound wave train such as caused by a passing vessel, if the fluid velocity is of the scale of H/T, then shorter waves in the train, with smaller T, will have a larger relative contribution to the fluid velocity than suggested by their apparent contribution to free surface disturbances, of scale H. This effect will decay more quickly down into the flow for shorter waves, as has been explained, but swimming animals, for example, in the upper part of the stream might experience a rather more "turbulent" time than surface disturbances suggest.

The quantity H/T has almost always been neglected, and this might help to explain the relative paucity of general results in this research area. Bhowmik et al. (1991) did calculate what they called the "steepness" H/T of each individual wave, but in the end this was not used, and they concentrated on the wave height H itself. Nanson et al. (1994) calculated the real wave steepness H/λ, where λ is the wavelength; however, they calculated λ from T using the deep-water formula $\lambda = gT^2/2\pi$. Possibly unsurprisingly, they found that their three erosion indices did not show a strong correlation with that H/T^2.

3.1.2 | Fluid velocity and the time derivative of surface height $d\eta/dt$

One disadvantage of just using H/T is that it is the scale of the velocity but actually not an approximation to the velocity, which is actually more like $\pi H/T$. Another disadvantage is that measuring a meaningful value of H and T for every wave in a record using wave-by-wave analysis is non-trivial, and can be arbitrary. There is, in fact, a simple measure of velocity that can be obtained from a record of surface elevation without having to identify individual waves. It requires no approximate wave theory and is approximately equal to the velocity at the surface for the usual case where waves are shorter than the depth.

Consider the non-linear kinematic boundary condition on the free surface $z = \eta$, one of the fundamental equations governing water wave motion (Dean & Dalrymple, 1991, equation 3.11c; Fenton, 2015, Section 4.2):

$$\frac{\partial \eta}{\partial t} + u_s \frac{\partial \eta}{\partial x} + v_s \frac{\partial \eta}{\partial y} - w_s = 0 \quad \text{on} \quad z = \eta, \tag{6}$$

where u_s, v_s, and w_s are the fluid velocity components at the surface in the x, y, and z directions respectively, with z and w_s vertical. The equation is exact and can be interpreted as requiring that particles on the free surface remain there.

Here, the reasonable local approximation is made that a wave is propagating without change in a direction x at velocity c, with no variation in the transverse direction y. The free surface elevation can be written as a function $\eta(t')$ of a time-like variable $t' = t - x/c$. To appreciate this, it helps to consider a downstream point $x + c\Delta t$ at a later time $t + \Delta t$, for which $t' = t + \Delta t - (x + c\Delta t)/c = t - x/c$, which is the same as the value of t' at point x at time t, hence the function $\eta(t')$ has the same value at both points, such that it describes a travelling wave.

Using the chain rule for partial differentiation, together with $\partial t'/\partial t = 1$ and $\partial t'/\partial x = -1/c$:

$$\frac{\partial \eta}{\partial t} = \frac{d\eta}{dt'}\frac{\partial t'}{\partial t} = \frac{d\eta}{dt'} \quad \text{and} \quad \frac{\partial \eta}{\partial x} = \frac{d\eta}{dt'}\frac{\partial t'}{\partial x} = -\frac{1}{c}\frac{d\eta}{dt'}. \tag{7}$$

Substituting into Equation (6) and considering the measuring point to be $x = 0$ such that $t' = t$, gives

$$\frac{d\eta}{dt} = \frac{w_s}{1 - u_s/c}. \tag{8}$$

That is, the derivative $d\eta/dt$, which is the apparent "velocity" of the free surface as it moves up and down, is equal to the local vertical fluid velocity w_s modified by a term $1 - u_s/c$, including the ratio of horizontal fluid velocity u_s to the wave speed c. That ratio is often small, such that $d\eta/dt$ is approximately w_s. For example, considering the common case of a shorter wave in deep water, kh large, Equation (2) can be written, using vector notation:

$$[u, w] \approx \pi \frac{H}{T} e^{kz} [\cos(kx - \sigma t), \sin(kx - \sigma t)], \tag{9}$$

showing that u has the same magnitude as w. Equation (1) gives $2\pi/T = \sigma \approx \sqrt{gk}$, from which also, as $c = \lambda/T = \sigma/k$ and setting $z = 0$ for the mean free surface, gives

$$\frac{[u_s, w_s]}{c} \approx \pi \frac{H}{\lambda} [\cos(kx - \sigma t), \sin(kx - \sigma t)]. \tag{10}$$

For the great majority of waves that are not breaking, H/λ is small, and so is u_s/c and so from Equation (8) $d\eta/dt \approx w_s$ is a satisfactory measure of the vertical velocity. Over much of the region intermediate between crest and trough, the cosine function is small and so is u_s/c. The value of H/λ for the highest wave in deep water is about 0.14, taking the limit $d \to \infty$ of equation (4.50) of Fenton (2015) and rounding the leading coefficient to two figures, so that near the crest of a high wave, when the argument of the cosine function is zero, Equation (8) gives $d\eta/dt \approx w_s/(1 - 0.14\pi) \approx 1.8\, w_s$, and near the trough of that wave, when the argument is π, $d\eta/dt \approx w_s/(1 + 0.14\pi) \approx 0.7\, w_s$. The factors 1.8 and 0.7 are not far from 1, and the mean value closer, even in this extreme case.

For short waves and/or deep water, as according to linear theory (Equation 9), the horizontal velocity u has the same magnitude as the vertical velocity w, in view of the above it can be concluded that for typical ship waves the magnitude of $d\eta/dt$ is a reasonable estimate of both components of the surface (maximum) fluid velocity, without any need for wave-by-wave identification.

Using $d\eta/dt$ does little to predict the fluid velocity down in the water, shown by Equation (9) to decay exponentially, the rate depending on the local wavelength. If one really needed fluid velocities near the bed, one would have to measure them there. However, for a measure of the magnitudes of fluid velocities, the quantity, $d\eta/dt$, easily calculated from a record of η, is a convenient quantity to express the velocity scale, possibly raised to the power 2, $(d\eta/dt)^2$, to give the magnitude of effects on the natural environment such as drag and shear forces. It provides a convenient basis for comparing different stressors and situations.

To perform the numerical differentiation, consider the record of a ship event with N measurements of surface elevation η_n, $n = 1, 2, \ldots, N$. For equally spaced intervals Δt, the derivative can be calculated from the central difference formula

$$\left.\frac{d\eta}{dt}\right|_n = \frac{\eta_{n+1} - \eta_{n-1}}{2\Delta t} \quad \text{for} \quad n = 2, \ldots, N-1\ . \tag{11}$$

Such numerical differentiation is, however, susceptible to noise in the signal. In the field study reported below in Section 4 it was found necessary first to smooth the sequence by first passing through all the readings and taking the local means of the values at five adjacent points (over a time interval of $5 \times 0.02\ \mathrm{s} = 0.1\ \mathrm{s}$). This was found to work surprisingly well, after comparison with results from a more complicated method using Fourier transforms with a cut-off filter.

3.2 | Water level extrema

Extrema of the water level, η_{max} and η_{min} are of environmental importance, determining how high the water can splash up on the banks, and how low is the exposure of the banks, whether short or long term, due to shorter waves or to drawdown. These quantities are trivially calculated passing through a record of surface elevation η_n, $n = 1, 2, \ldots, N$. No wave-by-wave analysis is necessary. Unlike the numerical differentiation, no smoothing was necessary in the field study reported below.

However, the connection between wave height and runup is far from trivial, even if the geometry of the bank is known. Wave runup is a complex and highly nonlinear process, including whether the waves are breaking or not.

3.3 | Identification and quantification of drawdown and other long-period surges

The third important quantity considered in the literature review for the effects of navigation on the environment, after fluid velocity and water level extrema, was the drawdown, that wave travelling with the ship due to its partial blockage, the higher velocity of the water around it, and the corresponding sinkage due to energy conservation.

In the previous studies reported above, although in principle it is easy, there was no mention of how drawdown was calculated, which seems a problem, given the presence of many shorter ship waves. Here an automatic procedure is proposed. Above in Section 3.1.2, to obtain values of $d\eta/dt$, it was recommended to obtain a simple local mean to smooth the sequence of measurements and eliminate local fluctuations of less than about 0.1 s. Longer means can also be used to smooth the sequence much more severely to reveal much longer waves and enable simple calculations to be done. In Section 4, it is described how local means over a time interval of 2.4 s were used, which again was found to work well. With such a smooth signal, effectively removing all short ship waves, it becomes relatively easy using point-by-point operations to determine maxima and minima and times when the signal passes through zero (mean water level) if that were desired to be the beginning and end of a drawdown event. This also allows the possibility of using alternative definitions of drawdown and surges such as between extrema, rather than between zeroes.

Bhowmik et al. (1981) wrote: "the extent of shoreline exposure and its duration might be of higher importance in bank erosion and biological studies than just the maximum drawdown value." An obvious extra quantity that can be calculated from surface elevation records is the time integral of the drawdown, thus compounding both extent and duration. Hence one might calculate, either for a positive or negative event, a surge or drawdown respectively,

$$\text{Integrated surge} = \int_{t_0}^{t_1} \eta(t)\,dt \approx \Delta t \sum_{n_0}^{n_1} \eta_n, \tag{12}$$

where subscripts 0 and 1 pertain to the beginning and end of the event, however that is identified, between extrema or zeroes, and we have been less than exact with the approximation at the end points, which are arbitrary anyway.

3.4 | Quantification of cumulative effect of waves in an event

Concerning the entrainment of bottom sediment or the detachment of organisms or nests maximum velocity will be an important quantity. However, the question of the combined effects of the entire wake of a vessel remains an open one. As described in the literature review, most investigations have incorporated some sort of measure of the cumulative effect of the waves, possibly in the form of mean wave height $\overline{H}$ or significant wave height H_s. Also different measures of the energy and/or power in the whole wave record have been calculated using linear wave theory and a wave-by-wave analysis, and then possibly combining with the group velocity, also from linear wave theory, to give a rate of transmission. Often this was found to be difficult by the requirement to define the wave train. A common step was then to ignore such results and consider just H_{max}. No one seems to have been certain.

Here we suggest two different measures of the effect of all disturbances in an event, neither of which uses wave theory, but both simply and directly use surface elevation measurements. Whereas they are plausible measures and simply obtained, their direct physical significance has not been established.

3.4.1 | Integrated effects of velocity—The "kinetic" integral

In view of our assertions above that it is velocity that is important such that H/T or $(H/T)^2$ are better expressions of environmental effects than H or H^2, it is possible that some progress could be made by calculating mean or significant values of those over a whole wave record and correlating with measured outputs such as turbidity. However, it is thought best to avoid the complications of wave-by-wave analysis. It would be simpler to use Equation (11) to give the directly-calculated velocity scale $\mathrm{d}\eta/\mathrm{d}t$ or its square $(\mathrm{d}\eta/\mathrm{d}t)^2$ and from them to calculate a time-integrated value as an overall stressor. We cannot, however, use the calculated value of $\mathrm{d}\eta/\mathrm{d}t$ integrated with respect to time over the whole wave record, as it is close to zero, simply being the difference between initial and final values of η. Remembering that effects on the environment such as drag forces and shear stresses for sufficiently large Reynolds number are usually proportional to the square of the velocity, the integral of the square of the velocity scale is suggested. We term this the

$$\text{“Kinetic” Integral}: \int_0^t \left(\frac{d\eta}{dt}\right)^2 dt \approx \frac{1}{4\Delta t}\sum_n \left(\eta_{n+1}-\eta_{n-1}\right)^2, \qquad (13)$$

where for the approximation to the derivative we have used the central difference formula (11), and for the integral we have used the trapezoidal rule, but here not being precise about the treatment of the arbitrary end points so that it is just a simple sum. Both approximations are simple and accurate enough. Importantly, no wave theory has been used.

The Kinetic Integral could be used as a measure of total environmental impact of the square of the velocity, where the upper limit of the integral would be the total time of recording of the event and the sum would be over all the measurements.

The calculation of *total* vertically integrated kinetic energy under the waves, however, would require knowledge of the whole velocity field, which is not feasible.

3.4.2 | Measure of surface disturbance—The "potential" integral

It is possible to calculate another quantity that is related to potential energy in the whole wave train and which also makes no use of approximate wave theory. In the previous section we just integrated a surface quantity in time. Here a more fundamental approach can be made. We consider the potential energy per unit plan area, relative to the bed, of a water column of total depth $h+\eta$, where h is the undisturbed depth and η the local water surface elevation due to a wave disturbance at any instant:

$$\mathrm{PE}/\mathrm{area}: \quad \frac{1}{2}\rho g(h+\eta)^2.$$

The value due just to the waves is then, subtracting the still-water value:

$$\mathrm{PE}/\text{area due to waves}: \quad \rho g\left(\frac{1}{2}(h+\eta)^2-\frac{1}{2}h^2\right)=\rho g\left(h\eta+\frac{1}{2}\eta^2\right).$$

Now we calculate the time-integrated value over a finite length of time t, the total potential energy per unit area that has passed a point to time t:

$$\text{Time-integrated PE/area due to waves} = \rho g h\int_0^t \eta \mathrm{d}t+\frac{1}{2}\rho g\int_0^t \eta^2 \mathrm{d}t. \qquad (14)$$

Over a number of waves the first integral will be close to zero as we have calculated the η such that $\overline{\eta}=0$. The remaining integral gives the time-integrated potential energy per unit area. Dividing that by $\frac{1}{2}\rho g$, we write what we call the

$$\text{“Potential” Integral}: \int_0^t \eta^2 \mathrm{d}t \approx \Delta t\sum_n \eta_n^2, \qquad (15)$$

approximating by summing over the squares of the surface elevations relative to the mean surface elevation recorded in that event. This also makes no use of wave theory and is simply obtained. The magnitude of the quantity as we obtained it from an energy consideration has little meaning, as it is not applied in a further calculation; our then dividing by $\frac{1}{2}\rho g$ gave this simple quantity with physical units. As no direct physical mechanism connecting energy and environmental impact has been proposed, it seems satisfactory just to use the numerical value of Equation (15) to compare the impact of different vessels at different sites and times, and indeed between studies. It could be interpreted as $\overline{\eta^2}\times t$ and if desired one could divide by t to give the mean square surface elevation. However, it is the totality that is a measure of impact.

For small amplitude waves, kinetic energy is equal to the potential energy (see, for example, Dean & Dalrymple, 1991, Section 4.7; Fenton, 2015, Section 4.4.6). As energy is conserved, the sum of the potential and kinetic contributions should be that experienced by all points along the side of the river, both along the stream, and transversely until quite close to shore when some dissipation will occur. Accordingly one assumes that the integral/sum in Equation (15) is relatively independent of measurement position, especially in view of the following section.

3.5 | Results independent of measurement position: Shoaling and refraction

As waves approach the shore they "feel" the bottom and will change in height as they shoal, that is, as the depth decreases, to maintain energy conservation. This means that measured height should depend on measurement position. However, it will now be shown that, surprisingly, this change of wave height is relatively small until the last moments of breaking. Hence, it seems not to be important where surface elevation η is measured, an advantage for the above suggestions for measurement and analysis relying on it.

In general, waves approach the bank at an angle, so that the waves refract, and the growth of wave height is dependent on the history of its propagation over the shoaling bottom. There is little that can be said in general or in simple terms about this wave refraction. As a first approximation it is assumed that waves approach the shore with their crests parallel to it and to the underwater bed contours. Linear wave theory can be used (see, for example, Fenton, 2015, Section 4.5). The ratio of wave height H to that in deep water H_0 is given as a function of h/λ_0, where λ_0 is the deep water wavelength (given in terms of wave period T as $\lambda_0 = gT^2/2\pi$) parametrically in terms of kh by the equations

$$\frac{H}{H_0} = \frac{1}{\sqrt{\tanh(kh) + kh\left(1 - \tanh^2(kh)\right)}}, \tag{16a}$$

$$\frac{h}{\lambda_0} = \frac{2\pi h}{gT^2} = \frac{kh\tanh(kh)}{2\pi}. \tag{16b}$$

To study the shoaling of a particular wave of period T and deep-water height H_0 for any particular dimensionless depth h/λ_0 one would solve Equation (16b) numerically to give a value of kh, and calculate the corresponding value of H from Equation (16a), and so on.

For physical appreciation, however, it is easier to consider the variation of relative wave height H/H_0 with the ratio of depth to wavelength $h/\lambda = kh/2\pi$, rather than using period. Figure 2 shows that relationship, from Equation (16a). If we consider decreasing depth in the form of h/λ, passing from right to left on the figure, it is surprising that waves do not feel the bottom at all until the relatively shallow depth of about $h/\lambda \approx 0.4$ when, surprisingly, but following from energy conservation, the wave height actually *decreases* until about $h/\lambda \approx 0.2$, the water depth one fifth of the length. After this minimum, the wave height increases. If we take as a guide for the effects of shoaling on wave height to be a limit of less than 10%, such that $H/H_0 \lesssim 1.1$, we find the effects of shoaling to be unimportant for $h/\lambda \gtrsim 0.08$, that is until a depth of only 8% of the wavelength, with the pleasant conclusion that, until very close to the shore, shoaling is unimportant. The measured wave heights at a point should be quite representative all over the sides of the stream, and it is not particularly important where they are measured.

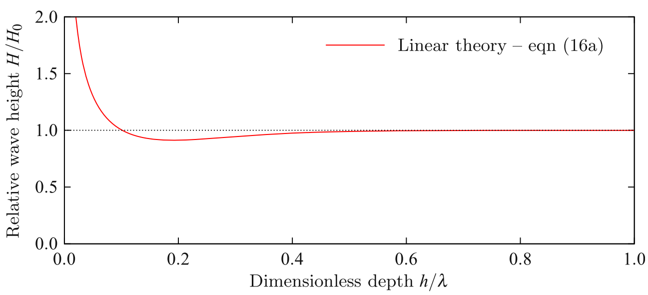

FIGURE 2 Variation of relative wave height H/H_0 with dimensionless depth h/λ [Color figure can be viewed at wileyonlinelibrary.com]

4 | A MEASUREMENT PROGRAMME ON THE DANUBE RIVER

4.1 | The nature of the river, sites, equipment, vessels, and analysis methods

East and downstream of Vienna the Danube is a regulated and navigable large-gravel-bed river. Some characteristic parameters are given in Table 1. The river is strongly influenced by a bedload deficit due to the damming and operation of hydropower plants upstream, thus the reach is incising (with rates averaged over the last decades between 2 and 3 cm p.a., Klasz et al., 2013), and there are other severe impacts because of inland navigation, both by traffic and by waterway maintenance and dredging. However, the river reach still shows major functional attributes of a natural river such as water level fluctuations, bedload transport, and associated biodiversity (Tockner, Schiemer, & Ward, 1998). In 1996, this reach and its floodplains became part of the Donau-Auen National Park. Subsequently in 2012 the Donau-Auen National Park administration contracted the engineering consultancy Gerhard Klasz and the Vienna University of Technology to measure ship-induced waves in the national park to identify those vessels that created the largest disturbances.

TABLE 1 Characteristics of the Danube River east of Vienna (Klasz, Reckendorfer, Baumgartner, Gabriel, & Gutknecht, 2013)

Drainage area	100,000	km^2
Mean annual discharge	1930	m^{3}s^{-1}
Mean annual flood	5,930	m^{3}s^{-1}
Estimated bankfull discharge	4,800–5,000	m^{3}s^{-1}
Median surface bed-material size D_{50}	20–25	mm
Bed-material size of which 90% is finer D_{90}	50–70	mm
Bankfull top width	350	m
Bankfull mean depth	5.75	m
Channel slope	0.00041	
Mean annual bedload	370,000	m^3 p.a.

The traffic volume situation at the time of the study could be estimated from the number of transits of the nearby locks at Vienna-Freudenau to be about 14,000 cargo and passenger vessel units per year (in both directions), and in addition there were about 900 passages by the Twin City Liners, fast (supercritical) catamaran ferries, travelling between Vienna and Bratislava. This resulted in an average of about 40 passage events per day. In the previous two decades a severe decrease of fish biomass from 247 to 87 kg/ha (BMNT, 2018) has been monitored, and the stress due to shipping (ship-induced waves) seems to be one of the most obvious reasons for that.

A series of field measurements was conducted on 1 and October 3, 2012 and 24 and July 25, 2013 in the Danube River, about 10 km east of Vienna, at two different sites, a flat bank (Site 1) and a steep one (Site 2), at 1909.95 and 1909.35 river-km respectively (origin at the mouth!). Figure 3 shows a plan of the area and the river cross-sections over a reach of 0.8 km encompassing the two sites. The variation, both longitudinal and transverse, is noteworthy.

A portable test rig of three 2 m long aluminium lattice girders was constructed, supporting an equilateral triangular array of three capacitance wave gauges with a spacing of 1 m. The signals of all three water level sensors plus a propeller meter were recorded at a frequency of 50 Hz. In the report to the National Park Administration, wave directions were calculated from the three signals. Here, only measurements from the outermost water level gauge are considered. Through preliminary tests it was found that the accuracy was about ±2.5 mm, with a very good frequency response. The measurements were of high quality and very few failures were found. For each passing ship, the details measured and recorded were: ship type, travel direction, distance from shore, and time. The data acquisition system *DoRis* of the operating company via *donau* was used with GPS data to identify the vessel and to determine its exact route as well as speed. Small speedboats could not be so identified. Water level recordings were made of 105 vessels and full data acquisitions were made for 93, including 21 high speed catamaran ferries, 5 hydrofoils, 12 small speedboats, 23 self-propelled motor barges, 12 push-tow-barge assemblies, and 20 passenger cruise ships.

In the original report, all records were analysed using Fourier methods, with smoothing to identify long-period components made using a numerical low-frequency filter. Although there were many experimental points, a total of some 5×10^6, with a mean of $N \approx 54{,}000$ in each record, Fast Fourier Transform software made the tasks feasible. In this present work it was found that such methods were not necessary, and any smoothing could be done by calculating local mean values. All necessary operations were performed using simple point-by-point numerical methods with a computational cost of order N. The total processing time of all vessels in the present study was several seconds.

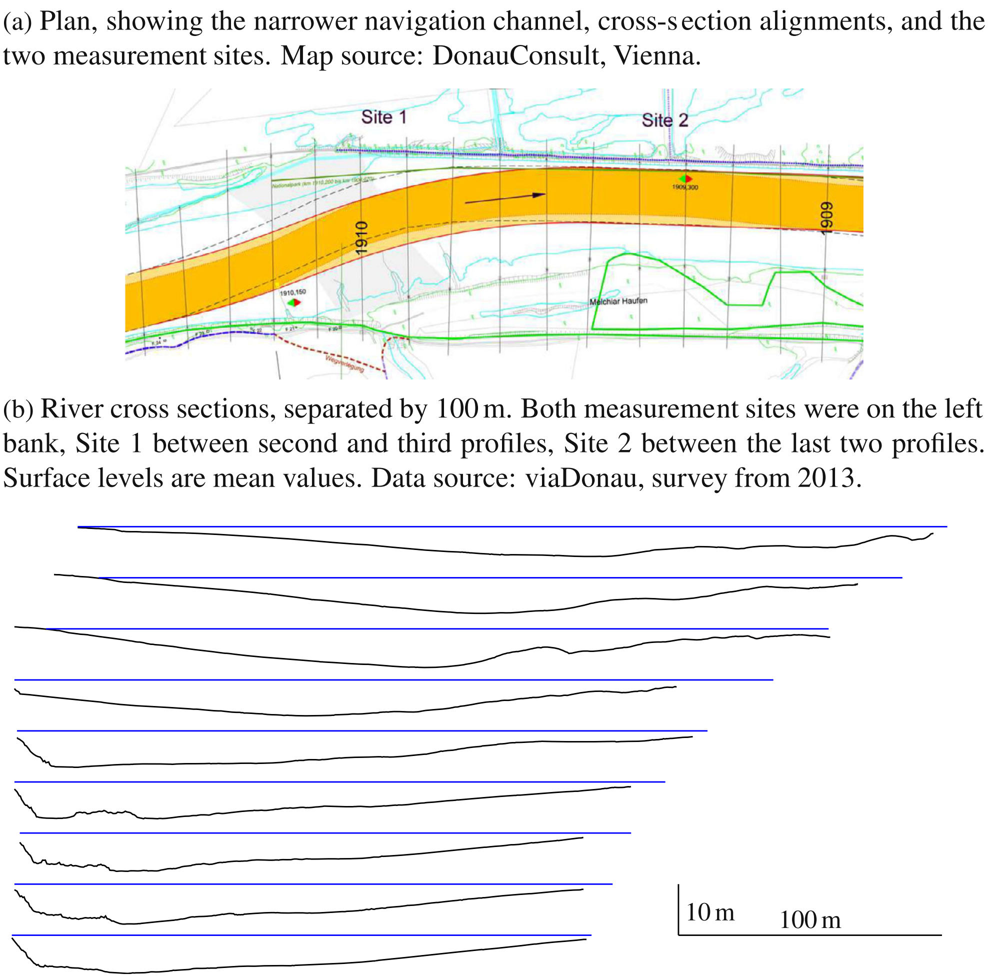

FIGURE 3 Physiography of the measurement reach [Color figure can be viewed at wileyonlinelibrary.com]

4.2 | Results for three different vessels

It is not the aim of this work to present detailed results of the types of waves and disturbances caused by all the ships, which was the object of the original report. Here the main purpose is to examine the quantities and methods presented in Section 3, to see how they perform. Different types of vessels have different primary and secondary wave systems. Figures 4–6 show quite different results from each of three very different types of vessel (Figure 5 from two identical vessels with closely similar results). They were chosen because each represented a common type and they showed the greatest values over all the ships of, successively, the velocity scale $d\eta/dt|_{\max}$, the range of surface level $\eta_{\max}-\eta_{\min}$, and the magnitude of the maximum integrated drawdown $\int \eta dt$.

In each figure, part (a) shows the actual measured record of the surface elevation η with no smoothing. A heavily smoothed record was also calculated using a local moving average of 121 points over an interval of 2.4 s to identify positive and negative surges, "drawdown" in the latter case. That is not plotted; what is shown are points where it passed through zero, easily calculated by a point-by-point process, with a view to a possible alternative definition of a surge event. In addition, the maximum and minimum water levels, also easily-obtained, are shown by horizontal dotted lines. In all three figures, the vertical scales of all parts (a) are the same, so that visual comparison between the three vessels can be made here; similarly the scales of the parts (b) are common to all.

The zero-crossings shown, and/or maxima of the smoothed record, either could be used as beginning and end points of surges to identify such events. An integral such as that of η shown in Equation (12) could be used to quantify them. Without the smoothing described here, such identification is problematical. Throughout the present work, it was attempted to develop automatic procedures, and in particular to avoid wave-by-wave analysis, as it is laborious and arbitrary in view of the many fluctuations that can occur. However, in this process of the identification of a long-period event, one is actually performing a surge-by-surge analysis. As the signal being operated on is much smoother, with fewer surges than individual waves, it is not so much a problem for computations.

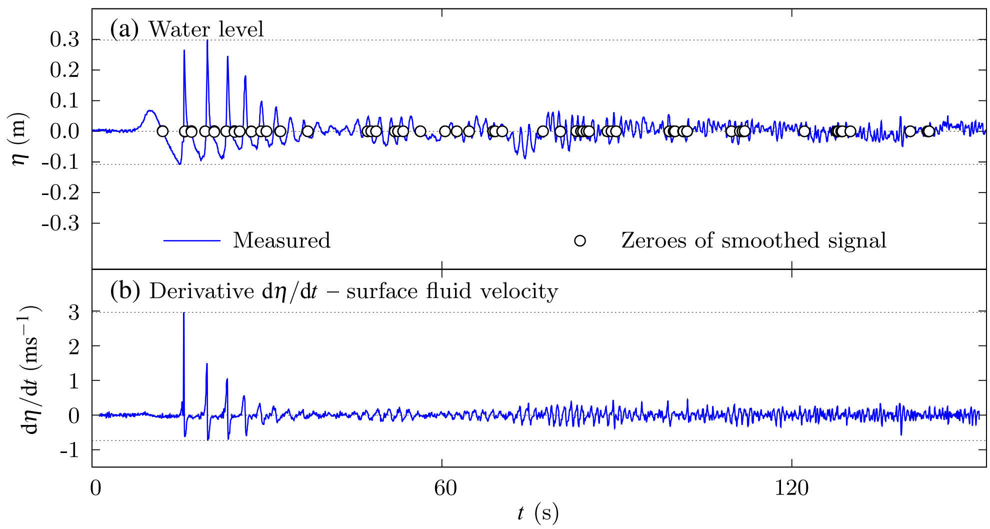

FIGURE 4 *Twin City Liner*, high speed catamaran ferry travelling downstream [Color figure can be viewed at wileyonlinelibrary.com]

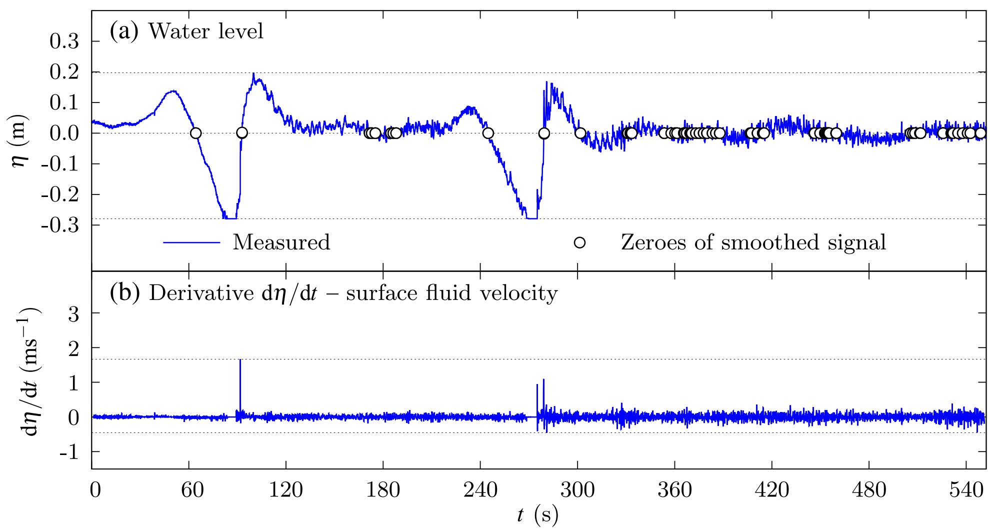

FIGURE 5 *MFS Amadeus Royal* and *MFS Amadeus Elegant*, twin passenger cruise ships, travelling slowly upstream [Color figure can be viewed at wileyonlinelibrary.com]

It is even simpler to use the integrals obtained in Section 3.4, giving single numerical values for the extent of velocity and free surface fluctuations. Part (b) of each of the figures shows a plot of the derivative $d\eta/dt$, which has been shown above to be a good measure of the surface fluid velocity. This was obtained by first smoothing the record using a moving average of five points over an interval of 0.10 s. This was necessary because there was a small oscillation in the height record at a period of about 0.3 s, unnoticeable in the η record as plotted, but giving irregularities in the $\mathrm{d}\eta/\mathrm{d}t$ result using Equation (11), an operation well known to be susceptible to noise. Also visible are the maximum and minimum values, shown by horizontal dotted lines .

Figure 4 *High speed catamaran*—: this vessel, a repeatedly-passing ferry, caused the largest short-period waves and fluid velocities. The heavily smoothed signal, shown in part (a) with a number of extraneous crossings is meaningless in this case, for there were almost no drawdown or significant surge events.

Figure 5 *Twin passenger cruise ships*—: possibly by coincidence, but more likely by operational planning by the company, this record shows the effects of two sister ships travelling at the same speed, the second 3 min after the first, a separation of only four ship lengths, relatively close to the shore and nearly line astern, with ship-shore ranges of 76 and 89 m. Of all vessels, they, and in particular the first, slightly closer to shore, caused the greatest difference between maximum and minimum water levels, shown in part (a).

Figure 6—*Push-tow with two barges placed trans*versely: this was a particularly bluff and slow-moving vessel combination. Part (a) shows that the drawdown was long, such that the bank was exposed for nearly 3 min.

4.3 | A tertiary wave system?

In the right halves of Figures 4–6 above, is something that was ubiquitous among the 93 events that we measured. After the passage of each ship and the primary and secondary waves, the river was brought to a high state of excitation, of "choppy" wave motion, of apparently random apparently short-crested waves. In the Danube measurement campaign, such waves continued for a long time, with little diminution by the time recording ceased, obvious in Figures 4–6. Other writers, described in the literature review, noted how difficult it was to define the end of an event. Figure 7 shows velocity records over an interval of 10 s close to the end of recording of each of the three ship events considered above. These later waves observed are smaller, but they are also shorter, such that the fluid velocities are still finite, something like 20–40 cm s^{-1}, although some vessels with smaller secondary waves had smaller continuing wave systems, with velocities more like 10–20 cm s^{-1}.

The explanation for the continuing wave system lies in the multiple reflections of waves from the shorelines of the river. It is well known that when periodic wave trains intersect at an oblique angle the result is a system of short-crested standing waves, little mounds of water bobbing up and down (e.g., Fenton, 2015, Section 4.4.4), and, of course, local fluid velocities oscillating correspondingly.

Figure 8 shows a mathematical solution to the ship wave problem obtained for an unbounded domain, the so-called "Secondary wave system". The representation here is, however, truncated at the river banks, and reflected waves shown, assuming as a first approximation that the reflection is perfect and the figure is drawn such that the reflected angle of each wave is equal to its angle of incidence. This shows the nature of the resulting wave system: that of two intersecting wave systems leading to short-crested waves propagating along and across the stream. In the frame of the ship, the system would be steady, with no change in time. However, in the stationary physical frame, the short-crested waves are unsteady, at any point the surface dancing up and down as the two systems of waves pass. What the figure hints at, but does not show, is that further upstream the whole river will exhibit the short-crested oscillations, after the reflected waves are themselves reflected from the opposite shore, and so on. More complicating is the effect of the nonlinearity of the governing equations generating harmonic shorter waves because of the interaction. If we consider a component of the incident wave being described by Equation (4) and other equations there are terms like

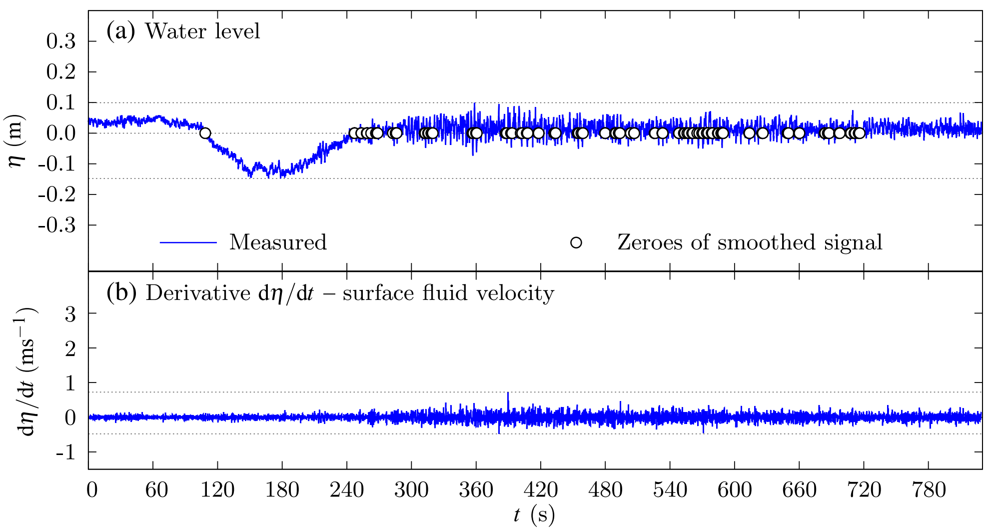

FIGURE 6 *MSS Ybbs*, large push-tow with two transverse barges, travelling slowly upstream [Color figure can be viewed at wileyonlinelibrary.com]

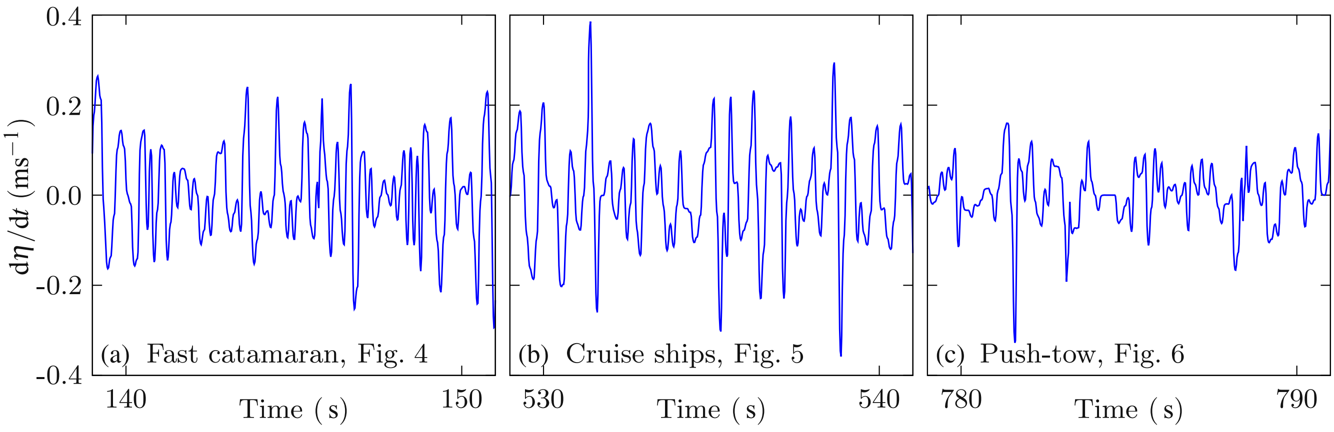

FIGURE 7 Surface velocity $d\eta/dt$ near ends of measurements [Color figure can be viewed at wileyonlinelibrary.com]

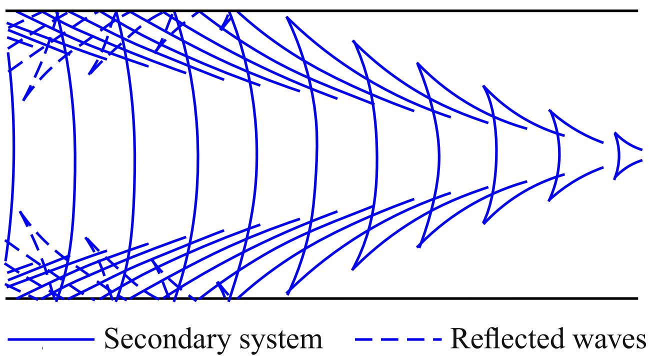

FIGURE 8 Secondary wave system and the effects of reflection from the banks beginning the process of turning the whole river into an irregular short-crested wave system [Color figure can be viewed at wileyonlinelibrary.com]

$H\cos(kx-\sigma t)$. If we consider the simplest quadratic non-linearity with a product of terms like that, we obtain $H^2\cos^2(\ldots)$, and from simple trigonometry, this gives a harmonic term with twice the frequency $H^2\cos 2(kx-\sigma t)$. Considering the full equations, we would see a large number of harmonic higher frequency contributions being generated. And, of course, more importantly in reality, the reflections from variable sloping banks are far from perfect with losses due to breaking so that the whole system is even more irregular.

An interesting extra deduction that can be made from the figure is that any measuring devices near the banks of the river, where they are usually placed, only momentarily experience purely secondary waves before any reflected waves start to contribute.

The effects of nonlinear reflections and interactions, leading to generation of harmonics, hinted at in the simplistic explanation above, is the possible explanation for what can be seen in Figure 7. In all three cases the oscillations have a shorter period than the constituent secondary waves, with roughly 15 cycles in the 10 s span, a wave period of only 0.67 s, and a radian frequency $\sigma = 2\pi/T = 9.4\ \mathrm{s}^{-1}$. Taking a deep water approximation to Equation (1), wavenumber $k = \sigma^2/g \approx 9\ \mathrm{m}^{-1}$ giving a wavelength $\lambda = 2\pi/k \approx 0.7$ m. The wave speed $c = \sigma/k \approx 1\ \mathrm{m\ s}^{-1}$, so that for a wave to traverse a distance of half the width of the river, very roughly 100 m (Figure 3), requires 100 s, and of course, a full crossing, 200 s. These figures are compatible with the results of Figures 4–6 and the hypothesis of generation by reflection from the banks.

In view of the different nature of the wave system, after the first and then multiple reflections leading to short-crested waves right across the river, the long duration with a large number of oscillations, and the suggestion that fluid velocity is important for organisms and possibly soil particles on the banks, this later wave system might have significant environmental impact. It is suggested here that it is distinct and important enough that it could be termed a *tertiary* wave system, following the primary and secondary wave systems generated by the vessels.

Another question is, why is there such an apparent enduring nature to such waves? We consider the expression for the viscous decay in time of periodic waves in deep water (Lamb, 1932, p624):

$$\frac{H}{H_{t=0}} = \exp\left(-2\nu k^2 t\right) = \exp\left(-2\nu\sigma^4/g^2 \times t\right), \tag{17}$$

where we have substituted the deep water approximation $k = \sigma^2/g$ from the large kh approximation to Equation (1). The decay coefficient is very strongly dependent on frequency σ. Inserting the values obtained above for typical tertiary waves, plus a representative value of $\nu = 1 \times 10^{-6}\ \mathrm{m^2 s^{-1}}$, for a full traverse of the Danube of roughly $t = 200$ s we find that the wave height is reduced by 4%, showing surprisingly little change, such that the effect of viscous dissipation is small. Wave breaking on the banks would be more important in reducing wave height, but this calculation goes some way to understanding the apparent durability of the tertiary wave system.

Of course, the fact that the tertiary waves are short means that their effects decay rapidly down into the water, in accordance with the theory presented above. In the short-wave limit, Equation (9) shows that the variation of velocity in the vertical is like $\exp(kz)$, so that for $k \approx 9\ \mathrm{m}^{-1}$ estimated above for tertiary waves, at a depth 10 cm below the surface the velocity is 40% of the surface value, for 20 cm it is 16% and for 30 cm, 6%. Any importance of tertiary waves would depend on the geometry of the situation, but these figures still show finite effects. More important might be wave action at the shore. If one examines the surface elevation records of the ships in Figures 4a–6a, one finds values of typical tertiary wave heights of, respectively, 10, 7, and 7 cm. These are small, however the effects of shoaling would increase them at the bank. The combined effect of the large number of such possibly-breaking events might be important.

4.4 | Measurement interval

To examine the necessary sampling frequency for ship wave measurements we considered our results for surface velocity $d\eta/dt$, as the act of numerical differentiation is more vulnerable to irregularities. Results from the high speed catamaran of Figure 4 are shown in Figure 9. Part (a) shows the large initial wave, and it is clear that rapid sampling of $\Delta t = 0.02$ s (50 Hz) is desirable; longer time intervals show diffusion in accordance with their magnitude. Part (b) at a later time apparently shows smaller secondary waves with a period of about 1 s; sampling at $\Delta t = 0.1$ s (10 Hz) is satisfactory, as the velocity is being described to within about 5% accuracy, while the $\Delta t = 0.20$ s results are not accurate enough. Part (c) for later shorter waves, that we assert are part of a tertiary system, shows that $\Delta t = 0.1$ s is no longer accurate enough. For an accurate determination of the velocities it seems necessary to measure at a rate of at least 20 Hz, $\Delta t \lesssim 0.05$ s.

4.5 | Compilation of results for all vessels monitored

Figure 10 is a summary of the results obtained from all of the vessels in the study, except for speedboats, whose paths were irregular and effects were small. It shows the five quantities: the vertical range of water levels $\eta_{max} - \eta_{min}$, the largest drawdown event from Equation (12), the "Potential" integral of η^2 in Equation (15), the maximum velocity scale $d\eta/dt|_{max}$, and the "Kinetic" integral of $(d\eta/dt)^2$ in Equation (13). The results are plotted in two columns of figures, in the left column for the vessel speed and second, on the right, the distance of the vessel from the shore. For simplicity, results for what are probably the other most important parameters, both shore types and both discharge levels, are not distinguished, as their effects were not great. In the case of each of the 10 cohorts comprising five types of vessel with two navigation directions, a linear curve of best fit is shown; any higher approximation would be overfitting.

4.6 | Vessel speed

Results from the leftmost five figures show the division of results into the two directions of navigation, unlabelled but obvious because of the speed ranges. In fact, there is little that can be deduced about the effects of vessel speed, because in almost all cases the vessels in each cohort travelled at about the same speed, nevertheless giving the wide range in dynamic effects measured. That required here the fitting of the lines using the vertical as the independent variable, otherwise the lines would have been short, nearly horizontal ones, near the vertical mean of each cluster. A wider range of speeds was found for passenger cruise ships travelling downstream, where all measures of wake increased with speed. For high speed vessels, the tendency of disturbances to decrease with speed is more explicable.

Part (b) of the figure for the maximum drawdown events shows how the three displacement vessel types, moving slowly upstream against the water flow, gave the largest integrated surface displacement, with the notable single largest case, the extreme one of the push-tow with two barges mounted transversely in Figure 6. The high speed vessels gave particularly little integrated surface displacement.

The other parts (a), (c), (d) and (e), considering overall water level fluctuations $\eta_{max} - \eta_{min}$, the fluid velocity scale $d\eta/dt$, and both the maximum value and the integral of the squares, show that the largest effects, could be caused by any of five of the six vessel types, the exception being hydrofoils. Notably, of the three types of slow-

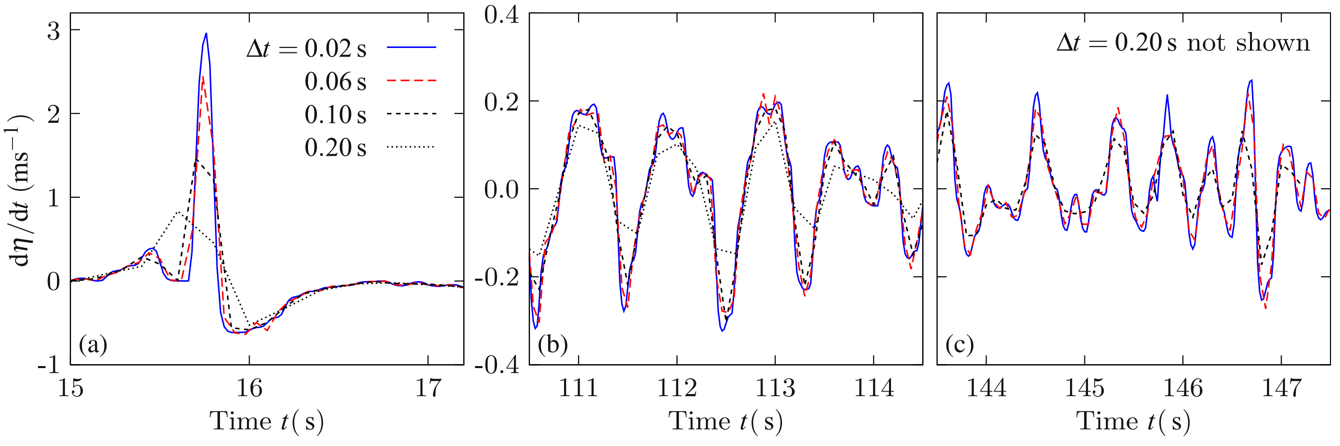

FIGURE 9 Effects of measurement interval. The vessel is the high speed catamaran whose results are shown in Figure 4. Part (a) is for the large initial wave, (b) and (c), drawn to different scales, are for later times, showing a transition from a secondary to a tertiary continuing wave system [Color figure can be viewed at wileyonlinelibrary.com]

moving displacement vessels, the most streamlined, the passenger cruise ships, created effectively just as much or more disturbance as the bluff commercial vessels.

4.7 | Distance from shore

To try to explain the considerable range of effects for much the same speed, consider the figures on the right of Figure 10, plotted against horizontal distance from the shore. There is a wide scatter of results but the mostly negative gradients of the fitted lines show that the range (distance from shore) is important, and that its effects generally decrease with distance, as might be expected. Considering integrated drawdown, shown in (b), this is also shown by results for the push-tow-barge assemblies. The other fitted lines, contrary to expectation, show a positive gradient, with drawdown increasing with range. However the scatter is large, and one can imagine almost-equally-valid near-vertical lines. There is some evidence, as experienced by a genre

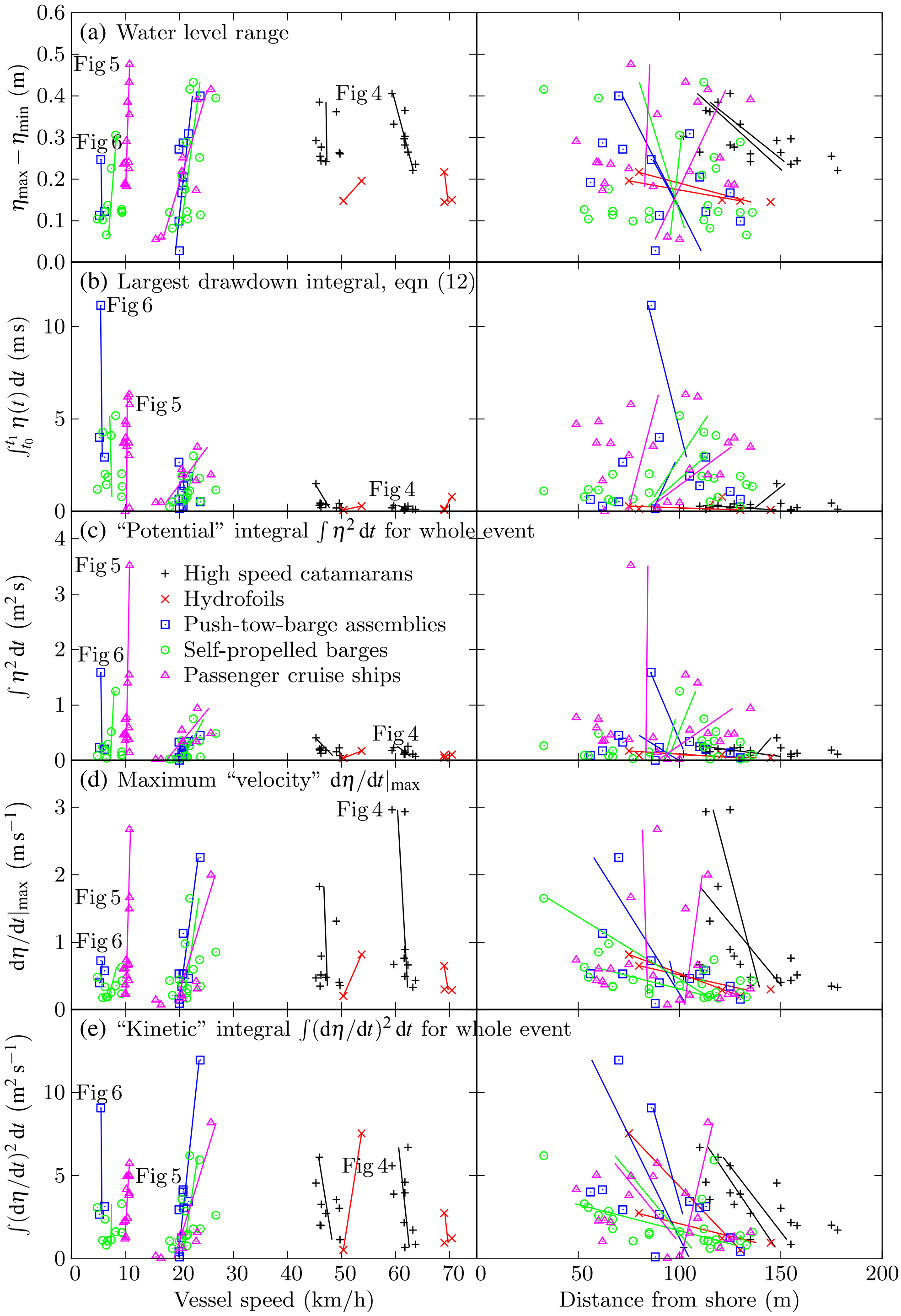

FIGURE 10 Summary of results, showing five different measures of impact and their variation with vessel speed and distance from shore. The key is in part (c); labels refer to figure numbers above [Color figure can be viewed at wileyonlinelibrary.com]

of video clips on the internet, that drawdown can still be large even when the vessel is some distance from the shore. It is possible that the drawdown has more of a two-dimensional nature than expected, so that instead of a vessel travelling in a local "basin" with the effect decreasing transversely away from the ship, the pattern is surprisingly simpler: the three-dimensional ship travels in a more two-dimensional trough across the stream.

It is clear that, like other studies of ship waves, here it has not been possible to generalise about the importance of various parameters. It is hoped that the methods developed here provide rational means of quantifying environmental effects, even if the problem of their prediction remains largely unsolved.

5 | CONCLUSIONS

A survey of the literature has shown that there are three effects associated with the wake of a ship that are important in determining its effect on the natural environment. They are (1) the fluid velocities and their effects on sediments, organisms living on or near the bottom, and swimming fish; (2) the sudden inundation and/or draining of stream banks leading to stranding or dislodgement; and (3) the longer-period exposure of the banks due to drawdown, leading to longer-term stranding.

Linear steady wave theory has often been used in the analysis of experimental results. That is a first approximation that can be used for understanding and insight, and for those purposes it has been used extensively here. For relatively high waves and irregular geometry it is not very accurate at all, and one can conclude that numerical results that have been deduced from it have often not been accurate. If that theory is used to infer surface elevations from sub-surface pressure measurements, the process has even more severe problems.

Where fluid velocity has been measured in the field, it has usually been at a single point, often at an intermediate depth. As it depends strongly on vertical position, the measured values might have had little connection with the environmental effects of the waves, especially on the bed.

Generally, however, it has not been velocity measurements that have been used to quantify the effects of ship events. Mostly, free surface elevation measurements have been performed, with wave-by-wave analyses, leading to the calculation of crest-to-trough wave heights and from them the compilation of quantities characteristic of the whole wave record. In fact, velocity has a scale given by H/T, the height of a wave H divided by its period T. That is only a scale, but it is a rather better measure of impact than just H itself which has been widely used in the past. As the force on organisms and stress on bed sediments are proportional to the square of the velocity for sufficiently large Reynolds number, the important quantity might actually be the second power $(H/T)^2$. To obtain values of velocity scale H/T requires a wave-by-wave analysis, which is often tedious and difficult. Instead, systematic procedures using surface elevation measurements have been proposed here. A simple method is given for calculating the vertical velocity at the surface from elevation measurements by calculating numerically the derivative $d\eta/dt$. Except close to the shore that vertical velocity is also the horizontal velocity. Down in the water the velocity can vary considerably and this method cannot help, however it gives a convenient method for rationally comparing the environmental impact of different vessels simply from the water level record.

In the case of longer-period motions, the velocity decays less with depth, and so has a greater effect on bed sediment. This explains the findings of other researchers that the movement of sediment and generation of turbidity are not caused by shorter waves but by longer-period ones.

It has been shown that shoaling and refraction of the waves are relatively unimportant until close to the shore, so that the placement of a water level probe in the horizontal plane is not critical.

Three different numerical integral quantities have been proposed here using the time series of surface elevation to express the overall impact of a ship event. To characterise the effects of drawdown, the integral of surface elevation in a drawdown event is proposed, Equation (12). This requires identification of the beginning and end of such a surge, for which recommendations are given. The other two integrals are evaluated rather more automatically. One, termed the "Kinetic" *integral* is the time integral of the square of the approximation to the surface velocity, $(d\eta/dt)^2$, Equation (13). This should give a magnitude to the overall effects of fluid velocity due to the waves. The other is the "Potential" integral, the time integral of the square of the surface elevation, η^2, Equation (15). This is directly related to the time integral of the actual potential energy due to the waves, and includes an integration over depth. The so-called "Kinetic" integral does not include that.

These techniques were applied to a measurement programme on the Danube River downstream of Vienna, comparing waves generated by different ships. It was found that except for hydrofoils, each of five different vessel types could cause roughly the same maximum surface fluctuations and similarly for the proposed integral quantities. Like other studies, a correlation of waves produced with the various navigation parameters was not definitive. The details of ship geometry and its wave and surge-making potential, which are usually not known, seemed to be most important. It was observed almost always that after the primary drawdown wave and the oscillatory secondary wave system, the river was brought into a state of oscillation with shorter less coherent waves but with finite fluid velocities that continued for a long time. The cause of this seems to be the reflections, initial and repeated, of the ship waves, leading to the whole river exhibiting short-crested wave oscillations. It is tentatively suggested that this is sufficiently environmentally important that it could be labelled a tertiary wave system.

The authors wish to thank the National Park Donau-Auen GmbH for funding the field measurements reported and applied in this study, DonauConsult of Vienna for permission to use the map in Figure 3, and viadonau - Österreichische Wasserstrassengesellschaft, especially Thomas Hartl, for providing survey data for that figure, and finally two expert referees who made important suggestions.

DATA AVAILABILITY STATEMENT

Research data are not shared.

ORCID

John D. Fenton https://orcid.org/0000-0001-5045-5968

REFERENCES

Almström, B., Roelvink, D., & Larson, M. (2021). Predicting ship waves in sheltered waterways – An application of XBeach to the Stockholm Archipelago, Sweden. *Coastal Engineering*, *170*, 104026.

Bhowmik, N. G., Demissie, M., & Osakada, S. (1981). Waves and drawdown generated by river traffic on the Illinois and Mississippi rivers, Research Report 271. Illinois State Water Survey.

Bhowmik, N. G., Soong, T. W., Reichelt, W. F., & Seddik, N. M. (1991). Waves generated by recreational traffic on the upper Mississippi river system, Research Report 117. Illinois State Water Survey.

BMNT. (2018). Sohlentwicklung in der freien Fliessstrecke unterstrom Kraftwerk Freudenau — Endbericht [in German], Technical report. Bundesministerium für Nachhaltigkeit und Tourismus.

Dean, R. G., & Dalrymple, R. A. (1991). *Water wave mechanics for engineers and scientists*. Singapore: World Scientific.

Fenton, J. D. (2015). Coastal and ocean engineering, Lecture notes. Vienna University of Technology. http://johndfenton.com/Lectures/Coastal-and-Ocean-Engineering/Coastal-and-Ocean.pdf

Fleit, G., & Baranya, S. (2021). Acoustic measurement of ship wave-induced sediment resuspension in a large river. *Journal of Waterway, Port, Coastal, and Ocean Engineering*, *147*(2), 04021001.

Fleit, G., Baranya, S., Krámer, T., Bihs, H., & Józsa, J. (2019). A practical framework to assess the hydrodynamic impact of ship waves on river banks. *River Research and Applications*, *35*(9), 1428–1442.

Fleit, G., Hauer, C., & Baranya, S. (2021). A numerical modeling-based predictive methodology for the assessment of the impacts of ship waves on YOY fish. *River Research and Applications*, *37*(3), 373–386.

Gabel, F., Garcia, X.-F., Brauns, M., Sukhodolov, A., Leszinski, M., & Pusch, M. T. (2008). Resistance to ship-induced waves of benthic invertebrates in various littoral habitats. *Freshwater Biology*, *53*(8), 1567–1578.

Gabel, F., Garcia, X. F., Schnauder, I., & Pusch, M. T. (2012). Effects of ship-induced waves on littoral benthic invertebrates. *Freshwater Biology*, *57*(12), 2425–2435.

Gabel, F., Lorenz, S., & Stoll, S. (2017). Effects of ship-induced waves on aquatic ecosystems. *Science of the Total Environment*, *601-602*, 926–939.

Göransson, G., Larson, M., & Althage, J. (2014). Ship-generated waves and induced turbidity in the Göta Älv River in Sweden. *Journal of Waterway, Port, Coastal, and Ocean Engineering*, *140*(3), 04014004.

Hofmann, H., Lorke, A., & Peeters, F. (2008). The relative importance of wind and ship waves in the littoral zone of a large lake. *Limnology and Oceanography*, *53*(1), 368–380.

Houser, C. (2011). Sediment resuspension by vessel-generated waves along the Savannah River, Georgia. *Journal of Waterway, Port, Coastal, and Ocean Engineering*, *137*(5), 246–257.

Klasz, G., Reckendorfer, W., Baumgartner, C., Gabriel, H., & Gutknecht, D. (2013). River-bed degradation and overbank deposition: A human induced geomorphic disequilibrium in the Donau-Auen National Park. In *Fifth symposium for research in protected areas, 10–12 June* (pp. 379–384). Austria: Mittersill.

Kucera-Hirzinger, V., Schludermann, E., Zornig, H., Weissenbacher, A., Schabuss, M., & Schiemer, F. (2008). Potential effects of navigation-induced wave wash on the early life history stages of riverine fish. *Aquatic Sciences*, *71*, 94–102.

Lamb, H. (1932). *Hydrodynamics*. Cambridge: Sixth Edition.

Liedermann, M., Tritthart, M., Gmeiner, P., Hinterleitner, M., Schludermann, E., Keckeis, H., & Habersack, H. (2014). Typification of vessel-induced waves and their interaction with different bank types, including management implications for river restoration projects. *Hydrobiologia*, *729*, 17–31.

Maynord, S. T. (2005). Wave height from planing and semi-planing small boats. *River Research and Applications*, *21*(1), 1–17.

McConchie, J. A., & Toleman, I. E. J. (2003). Boat wakes as a cause of river-bank erosion: A case study from the Waikato River, New Zealand. *Journal of Hydrology New Zealand*, *42*, 163–179.

Nanson, G. C., von Krusenstierna, A., Bryant, E. A., & Renilson, M. R. (1994). Experimental measurements of river-bank erosion caused by boat-generated waves on the Gordon river, Tasmania. *Regulated Rivers: Research and Management*, *9*(1), 1–14.

NIWA. (1998). At what depth should DOBIE be deployed?, technical note 98/1, NIWA Instrument Systems, Christchurch, New Zealand. https://niwa.co.nz/our-services/instruments/instrumentsystems/dobie/dobie_notes/dobie_tnote1

NIWA. (2001). Wave Gauge - NIWA DOBIE, Technical Note, NIWA Instrument Systems, Christchurch, New Zealand. https://niwa.co.nz/our-services/instruments/instrumentsystems/dobie/dobiedoc

Schludermann, E., Liedermann, M., Hoyer, H., Tritthart, M., Habersack, H., & Keckeis, H. (2014). Effects of vessel-induced waves on the YOY-fish assemblage at two different habitat types in the main stem of a large river (Danube, Austria). *Hydrobiologia*, *729*, 3–15.

Sorensen, R. M. (1997). Prediction of vessel-generated waves with reference to vessels common to the upper Mississippi river system, technical report ENV report 4. U.S. Army Corps of Engineers Waterways Experiment Station.

Tockner, K., Schiemer, F., & Ward, J. (1998). Conservation by restoration: The management concept for a river-floodplain system on the Danube River in Austria. *Aquatic Conservation: Marine and Freshwater Ecosystems*, *8*, 71–86.

How to cite this article: Fenton, J. D., Huber, B., Klasz, G., & Krouzecky, N. (2023). Ship waves in rivers: Environmental criteria and analysis methods for measurements. *River Research and Applications*, *39*(4), 629–647. https://doi.org/10.1002/rra.4101